






PLCL/PCL Dressings with Platelet Lysate and Growth Factors Embedded in Fibrin for Chronic Wound Regeneration

Johanka Tábořská¹ , Andreu Blanquer^{2,3} , Eduard Brynda¹, Elena Filová² , Lenka Stiborová¹, Věra Jenčová⁴ , Kristýna Havlíčková⁴, Zuzana Riedelová¹, Tomáš Riedel¹ 

¹Department of Chemistry and Physics of Surfaces and Biointerfaces, Institute of Macromolecular Chemistry, Czech Academy of Sciences, Prague, Czech Republic; ²Department of Biomaterials and Tissue Engineering, Institute of Physiology, Czech Academy of Sciences, Prague, Czech Republic; ³Departament de Biologia Cel·lular, Fisiologia i Immunologia, Universitat Autònoma de Barcelona, Bellaterra, Spain; ⁴Department of Chemistry, Technical University of Liberec, Liberec, Czech Republic

Correspondence: Tomáš Riedel, Institute of Macromolecular Chemistry, Czech Academy of Sciences, Heyrovského náměstí 2, 162 00 Prague 6, Czech Republic, Tel +420 296 809 333, Email riedel@imc.cas.cz

Introduction: The formation of diabetic ulcers (DU) is a common complication for diabetic patients resulting in serious chronic wounds. There is therefore, an urgent need for complex treatment of this problem. This study examines a bioactive wound dressing of a biodegradable electrospun nanofibrous blend of poly(L-lactide-co-ε-caprolactone) and poly(ε-caprolactone) (PLCL/PCL) covered by a thin fibrin layer for sustained delivery of bioactive molecules.

Methods: Electrospun PLCL/PCL nanofibers were coated with fibrin-based coating prepared by a controlled technique and enriched with human platelet lysate (hPL), fibroblast growth factor 2 (FGF), and vascular endothelial growth factor (VEGF). The coating was characterized by scanning electron microscopy and fluorescent microscopy. Protein content and its release rate and the effect on human saphenous vein endothelial cells (HSVEC) were evaluated.

Results: The highest protein amount is achieved by the coating of PLCL/PCL with a fibrin mesh containing 20% v/v hPL (NF20). The fibrin coating serves as an excellent scaffold to accumulate bioactive molecules from hPL such as PDGF-BB, fibronectin (Fn), and α-2 antiplasmin. The NF20 coating shows both fast and a sustained release of the attached bioactive molecules (Fn, VEGF, FGF). The dressing significantly increases the viability of human saphenous vein endothelial cells (HSVECs) cultivated on a collagen-based wound model. The exogenous addition of FGF and VEGF during the coating procedure further increases the HSVECs viability. In addition, the presence of α-2 antiplasmin significantly stabilizes the fibrin mesh and prevents its cleavage by plasmin.

Discussion: The NF20 coating supplemented with FGF and VEGF provides a promising wound dressing for the complex treatment of DU. The incorporation of various bioactive molecules from hPL and growth factors has great potential to support the healing processes by providing appropriate stimuli in the chronic wound.

Keywords: human platelet lysate, diabetic ulcer, fibrin coating, growth factors, nanofibers, bioactive dressing

Introduction

It is estimated that up to 2% of the population of developed countries will experience a chronic wound during their lifetime.¹ Therefore, there is an urgent need for complex wound treatments. A chronic wound (eg venous, arterial, traumatic, pressure, and diabetic ulcers) can be defined as a wound that has failed to proceed through a repair process.² Diabetic ulcers (DU) are a common complication for approximately 15% of all patients suffering from diabetes mellitus.³ DU not only cause serious lesions and abrasions that involve loss of epithelium but may also extend to the dermis and deeper layers, sometimes even involving bones and muscles resulting in the need for amputation.⁴ The hyperglycemic condition of diabetic patients hinders the wound healing process leading to a high risk of DU formation.⁵ Diabetic patients suffer from neuropathy development, reduced vascular healing capacity, glycation of hemoglobin that cause

hypoxia and the generation of reactive oxygen species (ROS) resulting in the breakdown of the extracellular matrix (ECM) in a wound leading to DU formation.⁵ A direct relationship has been attributed to the deficiency of growth factors (GFs) involved in the wound healing process (such as fibroblast growth factor (FGF), vascular endothelial growth factor (VEGF), and platelet-derived growth factor (PDGF-BB)). Wound healing is a complex process regulated by various signaling molecules, which involves cellular response and remodeling of ECM.

In current medicine, it is still challenging to enhance the DU healing processes by applying various wound dressings on the damaged area. An ideal wound dressing should mimic the properties of natural skin and fulfil specific functions, eg thermo-insulation and gaseous exchange, to help drainage and debris removal thus promoting tissue reconstruction processes, protection against infections, support of cell proliferation and migration, and support wound healing processes in general. Traditionally used gauze or cotton wool dressings serve mainly as protection for the wound against contamination, but lack other specific functions. Unlike traditional dressings, advanced DU dressings (hydrocolloids, hydrogels, foams, and films) aim to support the healing process via the sustained release of stimulating mediators, protection of bioactive constituents, enhanced protection against infection, or long-term drug release. These dressing materials are usually used in a combination of different synthetic and natural polymer-based biocompatible materials. Especially, nanofibers cast by electrospinning are widely used for their unique physical, chemical, and biological properties. Nanofiber scaffolds can mimic ECM and therefore are an ideal material for tissue engineering in the regeneration of damaged skin with a nano-sized structure and a huge surface-to-volume ratio.⁵ Moreover, nanofibers produced from biocompatible and biodegradable polymers are an ideal matrix that can have specific structural parameters (such as porosity, morphology, and surface area) with the possibility of modification for different applications. One of the most frequently used polymers is polycaprolactone (PCL). PCL has very good biocompatibility that can be further tuned in combination with other polymers, eg poly(L-lactide).⁶ Bioactivity of the material can be further improved by the attachment of various biomolecules such as peptides, extracellular matrix proteins, and growth factors.⁷ In this regard, a potential benefit can be achieved by the attachment of a complex matrix such as platelet lysate prepared from platelet-rich plasma.

Platelet-rich plasma is widely used in different medical fields, including wound treatment. It enhances the wound-healing process and tissue regeneration in chronic wounds by providing necessary growth factors and cytokines that stimulate the proliferation and differentiation of cells.^{8,9} Similarly, human platelet lysate (hPL) is a promising candidate for regenerative medicine. It is prepared from human platelet concentrate and is an excellent and universal source of various growth factors and cytokines promoting proliferation, migration and chemotaxis of different cell lines involved in the wound healing process.^{8,10,11} Exogenous addition of hPL has shown significant effects on cell migrations and proliferations both in vitro and in vivo.¹² However, the incorporation, stability, and gradual release of the hPL component from nanofiber membranes remains challenging.

Based on our previous results, we modified a blend of poly(L-lactide-co- ϵ -caprolactone) and poly(ϵ -caprolactone) (PLCL/PCL) nanofiber membranes (NF) with a fibrin coating (NF0) formed in a controlled manner. The fibrin coating is inspired by natural wound healing processes that lead to blood clot formation after a vascular injury. A blood clot, which contains a crosslinked fibrin mesh, activated platelets, erythrocytes, and leukocytes, is formed to stop bleeding and later serves as a temporary scaffold for cells and as a reservoir of GFs.¹³ The ability of fibrin to bind and retain GFs activity has been published previously.^{14,15} The fibrin coating was also shown to serve as an excellent substrate for cell growth on PLA nanofibers¹⁶ and on PLCL/PCL nanofibrous membranes.¹⁷ We previously reported that NF with fibrin containing 20% of hPL enhanced proliferation and differentiation of human keratinocytes.¹⁷ However, the rather low activity of incorporated growth factors from the hPL reduced the overall effect.

In this work, a biodegradable electro-spun blend of PLCL/PCL nanofiber membranes is used as a support layer (a platform) for a bioactive coating promoting chronic wound regeneration. The coating is based on a fibrin mesh prepared in a controlled manner containing hPL with addition of VEGF and FGF. The impact of the coating is verified on adult human saphenous vein endothelial cells (HSVECs).¹⁸ To mimic the natural environment and arrangement of the wound, the HSVECs are cultivated on a collagen layer and covered by the coated NF. We demonstrate that the hPL supplemented with growth factors and embedded in fibrin coated NF may become an advanced wound dressing to support the healing process by incorporating various bioactive molecules and stimulating HSVECs proliferation in the wound.

Materials and Methods

Material

Fibrinogen (Fbg) and Thrombin (Thr) from human plasma, Plasmin, TWEEN[®] 20, NaIO₄, NaOH, NaCl, CaCl₂, KCl, Na₂HPO₄·12H₂O, KH₂PO₄, Trizma[®] base, Dimethyl sulfoxide (DMSO), and Ethanol were purchased from Merck/Sigma-Aldrich (Darmstadt, Germany). Antithrombin III, S-2403 was purchased from Chromogenix (London, UK). Human fibroblast growth factor basic 154aa (FGF) and Human vascular endothelial growth factor 165 (VEGF) were purchased from GenScript (Piscataway, NJ, USA). Blotting-grade blocker was purchased from Bio-Rad (Hercules, CA, USA). VEGF human ELISA kit (KHG0111), FGF-2 human ELISA kit (KHG0021), PDGF-BB human ELISA kit (BMS2071), Micro BCA[™] protein assay kit, Fibrinogen polyclonal antibody (PA1-9526), Goat anti-Chicken IgY Alexa Fluor 488 (A11039), and Collagen I rat - tail were purchased from Thermo Fisher Scientific (Waltham, MA, USA). Human fibronectin ELISA kit (ab219046) was purchased from Abcam (Cambridge, United Kingdom). Cellvis glass bottom 24- and 96-well plates were purchased from IBL Baustoff+Labor GmbH (Gerasdorf, Austria). K-ASSAY[®]FIBRINOGEN protein kit was purchased from Kamiya biomedical company (Tukwila, WA, USA). HSVEC cells cat. no. 1210121 were purchased from Provitro (Berlin, Germany). EGM-2 (C-22111) was purchased from PromoCell (Heidelberg, Germany). CellTiter 96[®] AQueous one solution cell proliferation assay was purchased from Promega Corporation (Madison, WI, USA). Cell Counting Kit – 8 (CCK-8) was purchased from Dojindo (Rockville, MD, United States).

Phosphate-buffered saline pH 7.4 (PBS), Tris–HCl buffer 0.05 M with 2 mM CaCl₂ pH 7.4 (TB), Tris buffered saline (0.05 M Tris, 0.15 M NaCl; TBS) were filtered through a Millipore 0.22 µm filter.

Methods

Preparation of Nanofibers

The preparation of a blend PLCL/PLC nanofibrous membrane (NF) was described earlier.¹⁷ Briefly, the nanofibrous blend of poly(L-lactide-co-ε-caprolactone) (PLCL) and poly(ε-caprolactone) (PCL) was prepared by an electrospinning technique (Nanospider NS 1WS500U; Elmarco) at the Technical University of Liberec. The PLCL/PLC blend (1:1) of biodegradable polymers with ϕ 0.46–2.48 µm was prepared by mixing 5% of (w/w) PLCL (Purasorb PLC 7015, Corbion, Amsterdam, Netherlands) with 5% (w/w) PCL (PCL; Mn 80,000 g/mol; Merck, Darmstadt, Germany) in a chloroform/ethanol solution (8:2).

Sampling of the Nanofiber Membrane

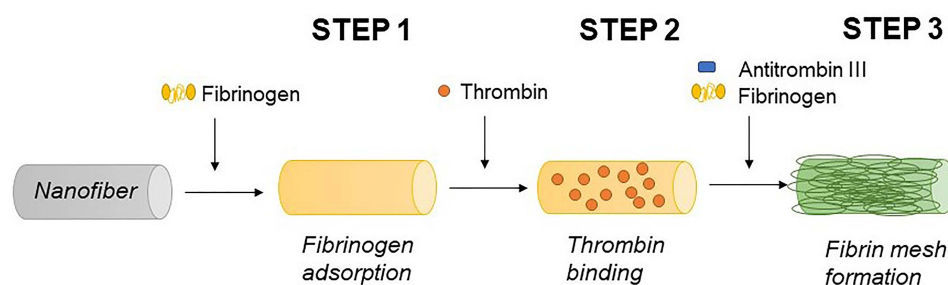
Circular samples (1.9 cm²) were cut from PLCL/PLC nanofibers. Samples were sterilized by immersion in 70% ethanol and UV light irradiation for 30 min. After sterilization, the samples were rinsed thoroughly and stored for 5 days in sterile q-H₂O to remove acid residuum prior to the coating process.

Human Platelet Lysate Preparation

Human platelet lysate (hPL) was prepared as described earlier.¹⁷ Briefly, platelets were separated as a buffy coat via centrifugation from 450 ± 45 mL of whole blood. Consequently, buffy coats from four different human donors were mixed and platelets were collected by low-speed differential centrifugation in solution which combined 70% of InterSol solution and 30% of blood plasma. Afterwards, the platelets were disturbed by a freeze–thaw method. The cellular debris was removed by centrifugation (5 min, 3,400 RCF; EBA 20, Hettich, Germany). After preparation, the platelet lysate was stored at –80°C. All donors agreed to participate in the study on the basis of informed consent.

Nanofiber Membranes Modification

The fibrin coating was based on our previously developed technique.^{17,19,20} The coating process consists of three subsequent steps. A schematic illustration of the coating procedure is depicted in [Scheme 1](#). Step 1; The surface of the NF was precoated with 5 µg/mL fibrinogen in Tris buffer (TB) in final volume 400 µL overnight at 4°C. Step 2; Following day, samples were rinsed with TB and a solution of thrombin 2 NIH U/mL in TB was added for 1 hour and then rinsed with TB.



Scheme 1 Coating procedure.

In Step 3, samples were incubated in a solution of 200 µg/mL fibrinogen and 0.25 U/mL ATIII (final concentration), and alternatively containing hPL and growth factors (GFs). The fibrin coating (NF0) was formed after 2 hours at RT. The coatings with hPL (labelled as NF1, NF5, NF10, NF20, and NF50) were prepared by the addition of a respective V/V (1, 5, 10, 20, and 50%) amount of hPL to the polymerization mixture. The NF100 coating was prepared by incubation of 100% hPL with the surface in Step 3. The hPL was normalized to the platelets count (100% hPL contained lysate of 634×10^6 platelets per mL). After polymerization, the nanofibers were gently washed three times with sterile PBS. NF20 coatings containing FGF and/or VEGF were prepared by the addition of 1 µg/mL of GFs into the polymerization mixture in Step 3 (NF20_{FGF}; NF20_{VEGF} or NF20_{FGF+VEGF}). Coated samples were used immediately after preparation unless otherwise stated.

NF Content Characterization

Protein Quantification

Coated NF were frozen and lyophilized (Gregor instruments, Czech Republic) immediately after preparation to prevent protein release/loss. A plasmin solution of 0.05 U/mL in PBS was added to lyophilized coated NF after preparation (labelled as T₀) as well as to coated NF after a one-week incubation in PBS (labelled as T₁₆₈) in order to release protein from NF into the solution. Samples were incubated with plasmin solution overnight at 37°C on a shaker (100 rpm; Unimax 1010, Heidolph Instruments, Germany). The final protein content on NF was calculated as a sum of protein released into the solution and remaining proteins on NF. The amount of protein was evaluated by Micro-BCA™ kit.

The amounts of growth factors (VEGF, FGF, PDGF-BB) and fibronectin (Fn) bound and released from coated NF were determined by respective ELISA kits (FGF/VEGF/PDGF-BB/Fn) following the producer's manual. The same ELISA kits were also used for the determination of FGF, VEGF, PDGF-BB, and Fn concentration in a stock solution of human platelet lysate.

Protein Release

Freeze-dried coated nanofibers were placed into a new 24-well polystyrene well plate with 400 µL of sterile PBS for protein release measurement. PBS was completely exchanged at 2h, 6h, 24h, 48h, and 168h time intervals. The amount of released protein was determined by a Micro-BCA™ protein assay kit following the producer's manual. The amount of released GFs and Fn was determined in the eluate by respective ELISA kit following the producer's manual.

Determination of Fibrinogen in hPL

Fibrinogen concentration in undiluted stock solutions of hPL was quantified by a K-ASSAY® FIBRINOGEN protein kit following the producer's manual.

Morphology of the NF Coating

Coated samples were incubated in a blocking buffer (TBS-T; 1% blotting-grade blocker in TBS+ 0.02% Tween 20) for 30 min; with fibrinogen antibody (1:1000; Thermo Fisher Scientific, PA1-9526) in TBS-T for 2 h; and with goat anti-chicken IgY Alexa Fluor 488 (1:2000; Thermo Fisher Scientific, A11039) in TBS-T for 1 h at RT. Finally, samples were

washed with PBS and kept at 4°C. Stained samples were observed using an Olympus IX83 confocal microscope (10x; 60x objective) and processed in ImageJ (1.53t) software.

Freeze-dried pristine and coated NF were sputtered with platinum and observed by SEM using a VEGA Plus TS 5135 microscope (Tescan, Brno, Czech Republic).

Inhibition of Plasmin Activity with hPL

Plasmin inhibition by hPL solution.

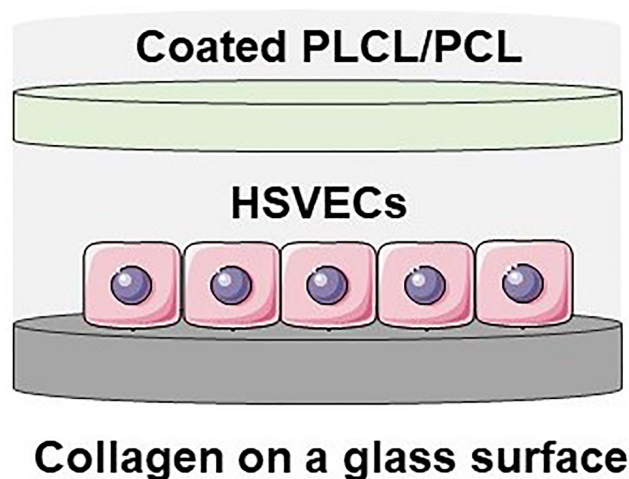
PBS as a reference, 20% hPL in PBS and 100% hPL, were incubated with chromogenic substrate for plasmin S-2403 (final concentration 0.4 nmol) and plasmin (final concentration 0.01 U/mL). The plasmin activity was measured by UV-VIS spectroscopy at 405 nm during a one-hour incubation in a 96-well plate. Absorbance was measured using a microplate reader (Epoch, Biotek, USA); data was collected every 40 seconds and the total sample volume was 150 μ L.

Plasmin Inhibition by Coatings

NF0, NF20 and NF100 were incubated with S-2403 (0.4 nmol) and plasmin (0.01 U/mL) in PBS (total volume 400 μ L) on a shaker (100 rpm) in the dark for 1 hour. Subsequently, 150 μ L of reaction solution was transferred into 96-well plate and the absorbance was measured at 405 nm and normalized to the NF0 (NF0=1).

Cell culture and cell viability

Primary human saphenous vein endothelial cells (HSVECs, passages 3-4) were used for cell viability evaluation. The cells were maintained in Endothelial growth medium (EGM-2) with supplements under standard culture conditions (37°C and 5% CO₂). The experiments were performed in low-supplemented EGM-2 containing 2% fetal bovine serum, heparin, ascorbic acid and hydrocortisone, without the presence of growth factors. In order to test coated NF in an arrangement as close to a DU dressing, NF were tested according to [Scheme 2](#) depicted below. NF were placed above cells (approx. 4 mm) and the HSVECs were cultivated on a collagen layer under coated NF. In this way, the effect of the coated NF on the viability, morphology and maturation of the HSVECs could be followed. Cell viability/metabolic activity was determined using CellTiter 96® AQueous One Solution Cell Proliferation Assay (MTS). HSVEC were seeded on a collagen coated 24-well glass bottom plate at a density of 20.000 cells per well. Prior to cell seeding, collagen (Collagen I, Rat tail) was deposited in a concentration of 50 μ g/ml in PBS on the plate overnight and subsequently washed by PBS. After 2 h of cell seeding, nanofibrous membranes were inserted into the cell culture well. The viability of the cells was measured after 1, 3, and 5 or 7 days in culture. NF were removed from the culture wells and cells were incubated with EGM-2 supplemented with MTS assay for 1 h. The absorbance was measured using



Scheme 2 Position of coated PLCL/PCL in cell culture experiments.

a VersaMax ELISA Microplate Reader spectrophotometer (Molecular Devices Corporation, Sunnyvale, CA, USA) at a wavelength of 490 nm, and normalized per well.

Cell morphology and maturation

Following the MTS assay, the cells were rinsed with PBS and fixed with 4% paraformaldehyde in PBS for 20 min. The morphology of the cells was analyzed via the staining of the actin filaments of the cells with phalloidin. For endothelial cell maturation, the von Willebrand factor was immunostained. In both cases, the samples were permeabilized with 1% of BSA in PBS containing 0.1% Triton X-100 for 20 min, and treated with 1% of Tween for 20 min at RT. The samples were then incubated with Atto 488-conjugated phalloidin (1:500; Sigma-Aldrich) for 20 min at RT. Alternatively, the samples were incubated with rabbit anti-von Willebrand primary antibody (1:400, Sigma-Aldrich, Merk, Darmstadt, Germany, Cat. No. F3520) overnight at 4 °C. After the samples had been rinsed twice with PBS, they were incubated with an Alexa Fluor 488-conjugated goat anti-rabbit secondary antibody (1:400). Images of the stained cells were captured under an IX-50 microscope (objective x 10) equipped with a DP 70 digital camera (both from Olympus, Tokyo, Japan). The intensity of immunofluorescence staining for von Willebrand factor in HSVECs was evaluated using the ImageJ software (ImageJ.org) and normalized per well.

Statistical analysis

The cell viability data and protein concentration data are presented as a mean with a standard deviation. Statistical comparisons were performed using one-way analysis of variance (ANOVA) with the Tukey's multiple comparisons test or by the student's one-tailed t-test. The analysis was performed using GraphPad Prism 9.1.1 (GraphPad Software, San Diego, CA, USA), and $p \leq 0.05$ was considered statistically significant.

Results and Discussion

Human Platelet Lysate Characterization

Platelets were collected from healthy donors and stored in a solution containing 70% InterSol and 30% blood plasma and disturbed by the freeze-thaw method to reach a platelet lysate. In order to avoid donor to donor variability in the platelet count, the platelet lysate (hPL) was standardized as a solution containing 634×10^6 platelets per mL. The concentration of selected biomolecules (fibrinogen (Fbg), fibronectin (Fn), platelet-derived growth factor (PDGF-BB), fibroblast growth factor (FGF), and vascular endothelial growth factor (VEGF)) was analyzed by immunoassays in hPL (Fbg 0.3 – 1.4 mg/mL; FGF 50 – 90 pg/mL; VEGF 50 – 100 pg/mL; PDGF-BB 10 – 16 ng/mL; Fn 35 – 45 µg/mL). The values were in agreement with previously published results showing hPL containing numerous bioactive molecules such as growth factors, pro-/anti-inflammatory mediators, and chemokines.¹⁰

Coating Preparation and Characterization

The fibrin-based coatings were prepared and characterized on an electro-spun blend of poly(L-lactide-co-ε-caprolactone) and poly(ε-caprolactone) nanofibrous membrane. PCL has a high degree of solubility in various solvents, satisfactory mechanical and biocompatibility properties, and a biodegradation ability which makes poly-ε-caprolactone polyester commonly used for fabrication of electro-spun scaffolds.²¹ The major disadvantage of PCL is the high hydrophobicity of the surface. This drawback was overcome by a combination of PCL with polylactic acid (PLA); a hydrophilic, biocompatible and biodegradable polymer. As a result, a PLCL/PCL blend with a higher degree of wettability was prepared.²² A PLCL/PCL blend nanofiber membrane (NF), with an average density of 22 g/m² and a thickness of approx. 25 µm, was produced with a well-defined fiber's diameter in the range of 400–800 nm. This tunable preparation of NF by electrospinning allows us to design versatile NF with small distances between singular fibers (an average pore size of 10.4 µm²) that would ideally protect a wound against extrinsic infection and simultaneously enable the exchange of gases and fluids.¹⁷

The NF were coated with fibrin in a controlled manner by a technique published previously (Scheme 1).^{17,19,20} The independent steps taken in this coating procedure allow us to control the morphology, thickness and homogeneity, as well as the reproducibility of the fibrin mesh formation on a surface.²⁰ Unlike the herein presented technique, conventional

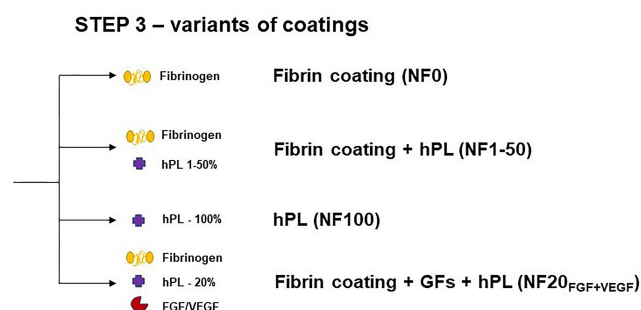


Figure 1 Variety of coatings on PLCL/PCL nanofibrous membrane.

methods of fibrin preparation that are based on the mixing of fibrinogen with thrombin, lead to a spontaneous, uneven, and unreproducible formation of a bulky fibrin mesh.^{20,23} Moreover, the bulky fibrin mesh has poor mechanical properties that limit its applications. Therefore, we chose a supporting layer based on electrospun PLCL/PCL nanofibers for the fibrin coating. We have already reported that the fibrin coating serves as a great substrate for cell growth on PLA nanofibers¹⁶ and PLCL/PCL nanofibrous membranes.¹⁷ In addition, the fibrin coating (referred as NF0) was enriched with hPL at different concentrations (v/v): 1% (NF1), 5% (NF5), 10% (NF10), 20% (NF20), 50% (NF50), and 100% (NF100); and by the addition of growth factors FGF and/or VEGF (Figure 1). Enrichment of the fibrin mesh with GFs and hPL is a key step in promoting the wound healing capability of the dressing. GFs as well as hPL have been shown to have great potential in wound healing.^{8,17}

The homogeneity of the fibrin coating was observed both by a scanning electron microscopy (SEM) and by a confocal microscope (LSM) after immunofluorescent staining (Figure 2). The NF0 coating homogeneously covered the surface of NF while leaving the inner parts of the NF free. By increasing the concentration of the hPL in the polymerization mixture the amount of visible fibrin mesh increased and reached a maximum for the coating containing 20% of hPL (NF20) and started to decrease at NF50 and NF100, where only some aggregates and artefacts were visible. The unmodified NF showed no fluorescence. In contrast to NF0, a dense surface confined fibrin mesh concealing the NF was formed on a NF surface with fibrin containing 20% of hPL (Figure 2). The thickness of the NF20 coating reached approx. 20–30 μm as measured by a confocal microscope.

To establish the optimal concentration of hPL in the final dressing coating, the total protein amount on the NF was analyzed by a BCA assay (Figure 2). In agreement with the confocal microscopy, the protein amount loaded into NF went up with an increasing concentration of the hPL in the range of 1%–20%, followed by a drop in the protein amount for coatings with 50% and 100% hPL (Figure 2A). This effect is most likely caused by the lack of Ca^{2+} ions in the ambient solution. Calcium ions are eliminated by the InterSol solution in which the platelets are separated and disturbed, and it prevents the spontaneous formation of a fibrin clot. These ions are crucial for the proper function of thrombin and therefore for the formation of the fibrin mesh. The highest protein amount was measured in NF20 (Figure 2A). The NF coated with 20% of hPL contained $354 \pm 67 \mu\text{g}/\text{cm}^2$ of protein. In line with our previous work where NF20 significantly stimulated keratinocyte growth,¹⁷ we focused on the NF20 more closely.

Stability of Coating Represented by Protein Release

The stability of the NF coatings was observed for one week in PBS (Figure 2). The analysis of the total protein residue in NF showed that almost 90% of NF20 content was released during one week (Figure 2B and C). The initial burst release of the protein into the solution was detected within 24 hours of preparation and was followed by a subsequent slow release of proteins from coated NF20 (Figure 2C). The initial burst release is probably caused by the most abundant and non-specifically attached plasma proteins like albumin.¹⁰ On the other hand, various molecules could be protected from the burst release by attachment to its specific binding sites on the fibrin mesh. Therefore, fibronectin (Fn) with its ability to bind to the fibrin mesh was used as a model protein to observe specific protein release from NF20.

The standard Fn concentration in blood plasma is typically up to 300 $\mu\text{g}/\text{mL}$.²⁴ The Fn concentration in the hPL was 40 $\mu\text{g}/\text{mL}$ (S.D. ± 5), which corresponds to the dilution factor of plasma during the platelet isolation. In the NF20 coating,

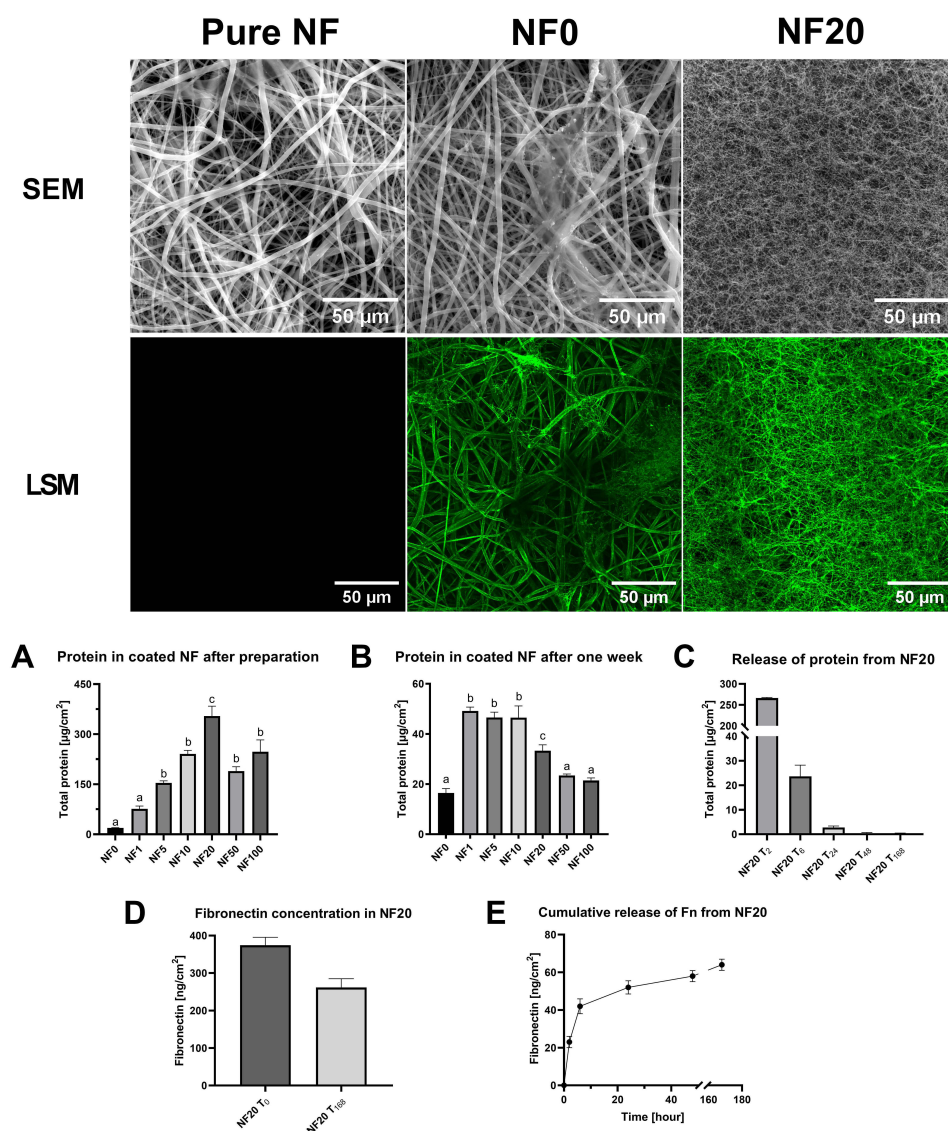


Figure 2 Characterization of coatings. Upper images represent uncoated (pure) NF observed by SEM; coated NF with the fibrin coating (NF0) and with the fibrin coating with 20% hPL (NF20) observed by confocal microscope (LSM). (**A** and **B**) Total protein concentration in the coated NF after preparation (**A**) and after one-week release into PBS (**B**); measured by BCA assay, ($n=6$) mean \pm SEM. The superscript letters above the columns (a, b, c) denote significant differences between the samples that do not share the same superscript ($p<0.05$). (**C**) Progress of protein release from NF20 measured from eluate by the BCA assay; ($n=6$) mean \pm SEM. (**D**) The graph represents concentration fibronectin in the NF20 coating after preparation (NF20T₀) and fibronectin level after one-week release (NF20T₁₆₈). (**E**) The graph represents cumulative release of Fn from NF20 for one week. D+E: Measured by ELISA, ($n=3$) mean \pm SEM.

we have detected 374 (S.D. ± 64) ng/cm^2 of Fn immediately after polymerization (Figure 2D) and the Fn release was monitored for one week (Figure 2E). Contrary to the burst release of non-specifically attached plasma proteins, only 11% of Fn was released within the first 24h into the solution followed by gradual release for the next week. After a one-week incubation, 262 (S.D. ± 40) ng/cm^2 of Fn remained in NF20, which is approximately 70% of the originally attached Fn. The result indicates that the fibrin mesh helps to preserve key components of hPL, such as Fn due to the presence of specific function domains and binding sites in its structure.^{25,26}

Fn has many important roles in the process of wound healing by interacting with different cell types, cytokines and the extracellular matrix (ECM). The pivotal role of Fn is in ECM formation during which the plasma Fn together with the fibrin mesh forms a provisional fibrin-fibronectin matrix that will later be replaced by the mature ECM-containing tissue Fn.²⁵ Fn has been found to significantly improve wound healing in irradiated skin²⁷ as well as significantly accelerate full-thickness skin wound closure in diabetic rats.²⁸ Gradually released Fn from the NF20 coating might be attached to the newly formed ECM in a wound, which is produced by fibroblast, and support cell migration.

Effect of hPL on Plasmin Activity

Wound healing is an overlapping biological process including fibrin mesh formation as well as fibrinolysis by plasmin. An uncontrolled fibrinolysis will lead to fibrin degradation followed by the subsequent release of attached bioactive molecules. In an attempt to simulate DU conditions, the NF0 and NF20 samples were incubated in the presence of plasmin (10 mU/mL) for two and five days (Figure 3A and B). The experiment revealed that plasmin accelerated the release of protein from the bare fibrin mesh. This effect was particularly visible for the fibrin coating that is otherwise stable in PBS (Figure 3A). After two days almost half of the NF0 coating was degraded by the plasmin. In contrast, nonsignificant differences in the degradation were obtained for NF20 incubated with plasmin for 48h (Figure 3B). This may be caused by a natural presence of plasmin inhibitors in the hPL such as $\alpha 2$ -antiplasmin. The $\alpha 2$ -antiplasmin is the main physiological plasmin inhibitor present in plasma.²⁹ Moreover, the $\alpha 2$ -antiplasmin has a very high affinity to the fibrin mesh³⁰ and is being crosslinked to the fibrin mesh during polymerization by FXIIIa, which is also present in plasma.²⁹ This inhibitor might reduce the degradation of NF20, prolong the stability of the NF20 coating in the presence of plasmin and provide a long-term delivery of bioactive molecules incorporated in the fibrin mesh. The presence of $\alpha 2$ -antiplasmin in NF20 was confirmed by mass spectroscopy (data not shown).

Plasmin is the major fibrin-degradation protease and it is naturally present in the wound exudate where it has been transported as a plasminogen by blood during the early wound healing process.³¹ Various plasmin activity (6–20 mU/mL) was detected in venous leg ulcers.³² Therefore, we chose 10 mU/mL of plasmin as an adequate model to study the fibrinolysis of the fibrin coating. Plasmin together with other ECM-degrading proteases (such as metalloproteases) initiate fibrin degradation and ECM remodeling.³¹

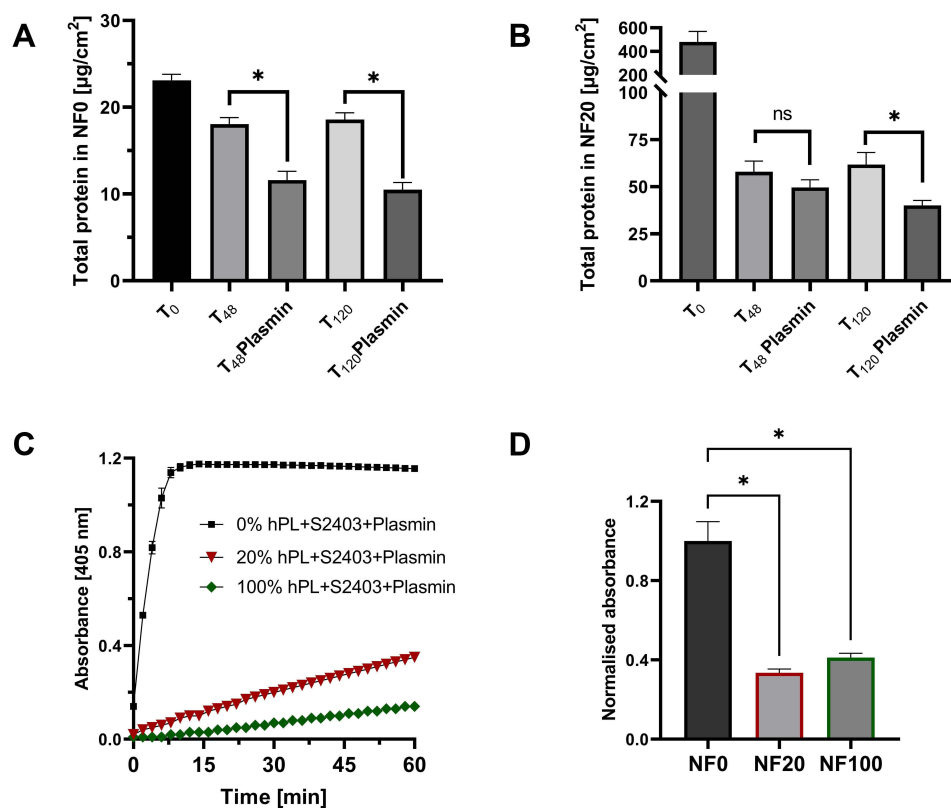


Figure 3 Inhibition of plasmin (10 mU/mL) by human platelets lysate. (A and B) Comparison of protein residuum in NF coated with NF0 (A) and NF20 (B). Coated NF were incubated with and without plasmin in PBS for 48- and 120- hour at 37°C. Mean \pm S.D., (n=3), evaluated by the student's one-tailed t-test. (C) Detection of an increase of absorbance for 1 hour in PBS (0%) and platelet lysate (20%; 100%; v/v) solution with plasmin and plasmin substrate S-2403; Mean \pm S. D (n=3). (D) Coated NF were incubated in a solution containing plasmin and S-2403 and an increase of absorbance was measured after 1 hour and normalized to NF0 (NF0=1); Mean \pm S. (D) (n=3) evaluated by the student's one-tailed t-test. *Shows statistical significance compared to control $p < 0.05$; ns – shows non-significant result.

The inhibition effect of hPL on plasmin activity is also illustrated in Figure 3C and D. The presence of α 2-antiplasmin greatly decreased the ability of plasmin to cleave a plasmin substrate S-2403 in solution and prevented the formation of a color product (Figure 3C). Non-diluted hPL had a stronger inhibition effect on plasmin than 20% hPL in solution. A slow and gradual increase in the absorbance shows that the inhibition was not ultimate, while in the control sample without hPL (0% hPL) a fast increase in absorbance was observed and saturation was reached after 7 min. Similarly, NF20 and NF100 coatings significantly decreased plasmin activity (Figure 3D); a higher inhibition effect was observed for NF20. This is in line with previous results which showed higher protein in NF20. These results provide important insights into the capability of plasmin to gradually release bioactive content from coated NF and the improved coating stability in the presence of plasmin.

FGF and VEGF Enrichment and Their Release

Coating of the NF with fibrin and hPL enables the specific attachment of various biomolecules and their accumulation in the fibrin mesh, including GFs. The NF20 coating contained 16.7 ± 1 pg/cm² of PDGF-BB after preparation. However, the insufficiently low levels of FGF and VEGF in hPL offer a possible therapeutic window for the external application of a GF to the wounds. In particular, a combination of VEGF and FGF has a strong synergic effect on tissue regeneration. In our previous study, we showed that the NF20 coating had a significant positive effect on cells proliferation.¹⁷ However, the initial concentration of the VEGF and FGF in the hPL was very low and undetectable in the coating. Therefore, in this study, we have supplemented the hPL with FGF and/or VEGF (1 μ g/mL) in order to further accelerate cell stimulation. The concentration and release rate of VEGF and FGF were subsequently measured (Figure 4A). Almost 40 ± 15 ng/cm² of VEGF was detected in NF20_{VEGF}, and 2.8 ± 1 ng/cm² of FGF was detected in the NF20_{FGF} coating after preparation (Figure 4A). Such a difference agrees with our previous report where an approx. 10 times higher amount of VEGF was attached to the fibrin coating than FGF.¹⁹ In addition, the combination of FGF and VEGF (NF20_{FGF+VEGF}) did not affect their attachment to the fibrin mesh.¹⁹ The results showed similar values for FGF and VEGF when they were added simultaneously.

Within the first day, we observed a fast release of the attached GFs, around 70% of FGF and around 90% of VEGF was released (Figure 4B). However, a more gradual release of FGF and VEGF was detected for the next seven days. After one week 493 ± 253 pg/cm² of FGF and 727 ± 178 pg/cm² of VEGF were still present in the coating. A similarly released kinetic has been described on poly(ether)urethane nanofibers with electrospun/sprayed fibrinogen containing hPL.³³ This scaffold showed a fast release of VEGF and PDGF-BB on day 1 and a gradual release for the next 7 days.³³ Sustained and long-term delivery of GFs into the wound is important to accelerate its healing.

Furthermore, the binding of GFs (eg VEGF, FGF, PDGF) to their natural binding sites on the fibrin mesh is known to improve their stability and activity.^{15,26,34} The half-life of unbound GFs is typically short; eg the half-life of VEGF in plasma was determined to be only 30 min.³⁵ It is expected that specific interaction with fibrin will help to maintain their biological activity and to protect them against degradation.³⁴

VEGF was reported to enhance endothelial cell migration, it plays a crucial role as a navigator for cells into hypoxia tissue, and has a pivotal role in cell proliferation and stimulates angiogenesis.^{35,36} Full-thickness skin wounds of diabetic mice treated with VEGF demonstrated significantly accelerated repair in VEGF-treated wounds.³⁷ VEGF not only stimulates neo-angiogenesis but also supports healing by a significant up-regulated expression of PDGF-BB and FGF in VEGF-treated wounds, which corresponds with the increased amount of granulation tissue in the wound.³⁷ PDGF-BB was shown to have a role in the structural integrity of the newly formed vessels by recruiting pericytes and smooth muscle cells to newly formed capillaries.³⁸ Moreover, human recombinant PDGF-BB (becaplermin) was approved in 2005 by the Food and Drug Administration (FDA) and is used under the trademark Regranex[®] as a gel-based topical treatment for DU. Furthermore, co-delivery of VEGF and PDGF-BB has been shown to expand the therapeutic window of VEGF and also improves associated arteriogenesis.³⁹ Although topical application of VEGF had a positive effect on the healing of diabetic foot ulcers in a first phase trial,⁴⁰ other trials reported no clear evidence of a difference between VEGF and placebo treatment.⁴¹

FGF has the potential to accelerate wound closure by activating cells such as vascular endothelial cells or fibroblasts and has a positive effect on the formation of granulation tissue.³⁶ The healing of full-thickness skin wounds was greatly improved when diabetic mice were treated with combinations of PDGF-BB and FGF.⁴² Also, significantly faster wound healing with FGF was observed on patients receiving topical FGF.⁴³

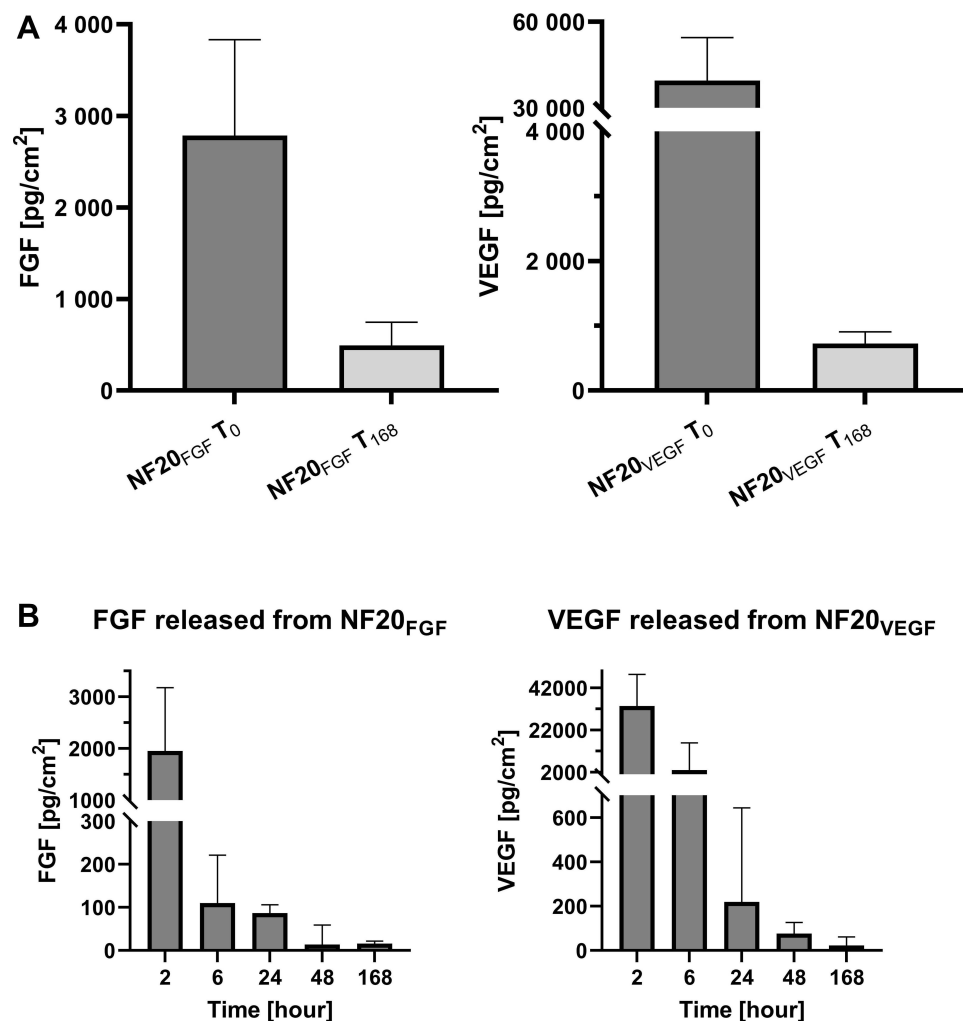


Figure 4 (A) Concentration of FGF and VEGF in NF20_{FGF} and NF20_{VEGF} after preparation (T₀) and after one-week (T₁₆₈). **(B)** Release of FGF and VEGF from coated NF20_{FGF} and NF20_{VEGF} into PBS. Measured by ELISA, (n=5) Mean ± SEM.

Cell Viability

The impact of fibrin-based coatings was verified on adult human saphenous vein endothelial cells (HSVECs). The HSVECs were cultivated on a collagen layer under floating coated NF (Scheme 2). This model mimics more closely the natural environment and the arrangement of a wound with a dressing than direct cultivation of cells on NF. To determine the effect of various coatings with different concentrations of hPL, the metabolic activity/viability of cells was quantified over time and the morphology of HSVECs was analyzed via the staining of actin fibers. Figure 5 shows cell response to coated NF with six different concentrations of hPL. After the first day, no significant differences were observed. The lowest viability was obtained for the NF100 coating. On the 3rd day, the highest viability was observed for the cells cultivated with NF10 and NF20, and significantly differed from the other coatings. On the 5th day, the viability assay of the cells under the NF20 coated PLCL/PCL membrane showed significantly stimulated cell growth compared to uncoated NF and coated NF with other concentrations of hPL. This finding is in line with our previously discussed result, which showed the highest concentration of protein in the NF20 coating (Figure 2). The additional increase of a hPL concentration up to 100% did not improve cell viability (Figure 5). In terms of cell morphology, the cells with the NF20 coating were well spread and closely packed, while no clear differences were observed between the other samples. In general, the cells adhered to the collagen layer and spread normally. The differences observed were linked to the number of cells, which correlated with metabolic activity results.

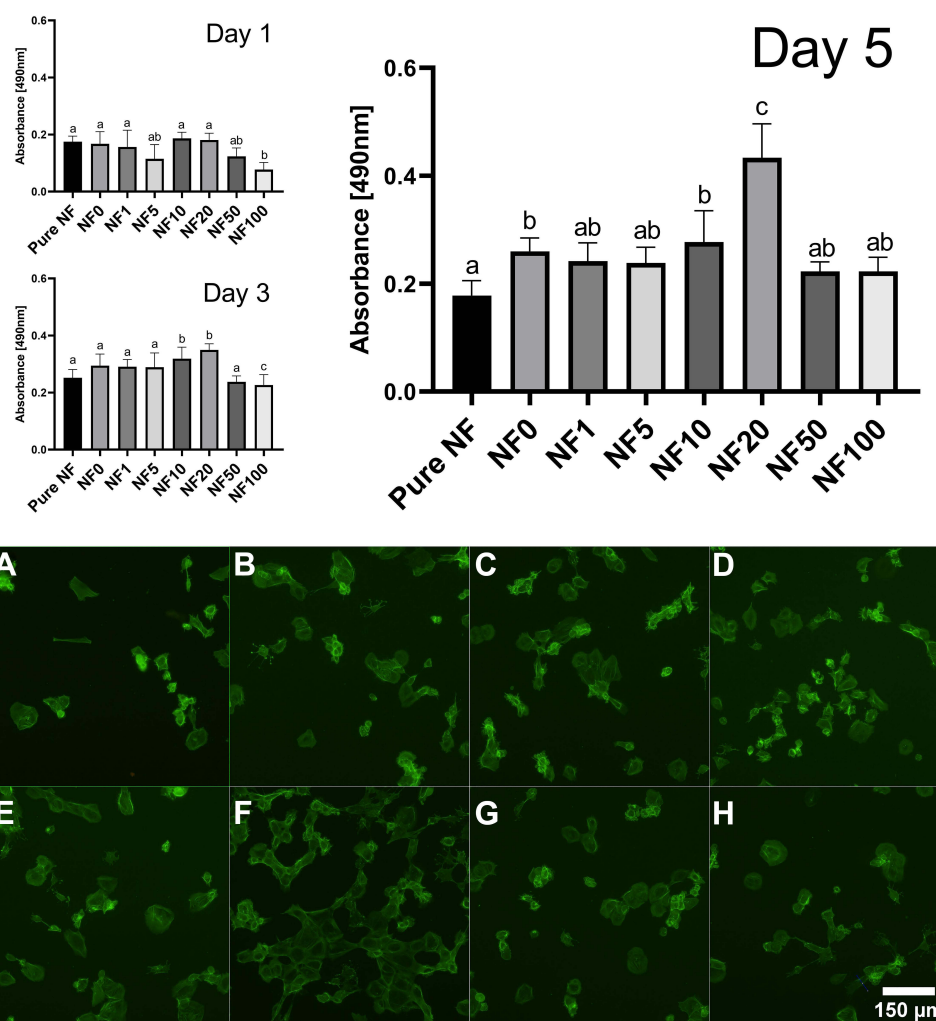


Figure 5 Stimulation of cell growth by human platelet lysate (hPL). The graph represents the cells' metabolic activity/viability measured after 1, 3, and 5 days in presence of NF coated with hPL in different concentrations (v/v). Mean \pm S.D. (n=6). The superscript letters above the columns (A–C) denote significant differences between samples that do not share the same superscript ($p < 0.05$). The cells cultured with pure NF (A), NF0 (B), NF1 (C), NF5 (D), NF10 (E), NF20 (F), NF50 (G) and NF100 (H) were stained with Atto 488-conjugated phalloidin (green); observed under the Olympus X71 microscope.

One limiting factor which impairs DU healing is inadequate blood supply that limits the transport of oxygen, antibiotics, and other molecules/immune cells into DU. Under normal conditions, hypoxia leads to the migration of microvascular endothelial cells into a wound to form blood capillaries. Hypoxia is also a trigger for hypoxia-stimulated VEGF expression. VEGF attracts cells and stimulates angiogenesis.⁴⁴ However, a diabetic patient has adversely attenuated VEGF production via impaired activation of hypoxia-inducible factor-1.⁴⁵ Fibroblasts isolated from diabetic patients as well as normal fibroblasts from healthy donors are defective in their capacity to up-regulate VEGF in response to hypoxia after exposition to high glucose.⁴⁵ Hence, a topical administration of VEGF via a dressing might be a way to overcome the lack of VEGF, thus promoting the closure of chronic wounds exhibiting hypoxia and compromised vascularity, and improve the healing ability of the DU.

Therefore, in this study we supplemented the NF20 coating with FGF and/or VEGF in order to further accelerate cell stimulation and proliferation. The effect of the exogenous addition of GFs was evaluated by the metabolic activity/viability assay and by fluorescent microscopy after immunofluorescence staining of the von Willebrand factor. The viability assay revealed a significant effect of the combination of both GFs already after 1st day (Figure 6). The same combination of GFs remained significant versus NF, NF20 and NF20_{VEGF} after 3 and 7 days. A positive effect of FGF was also visible after 3 and 7 days and the cell viability was comparable to the NF20_{FGF+VEGF} coating. On the other hand, the effect of VEGF alone did not show any significance in the cell viability assay. Despite this, we believe that VEGF might help in further in vivo tests to attract cells into

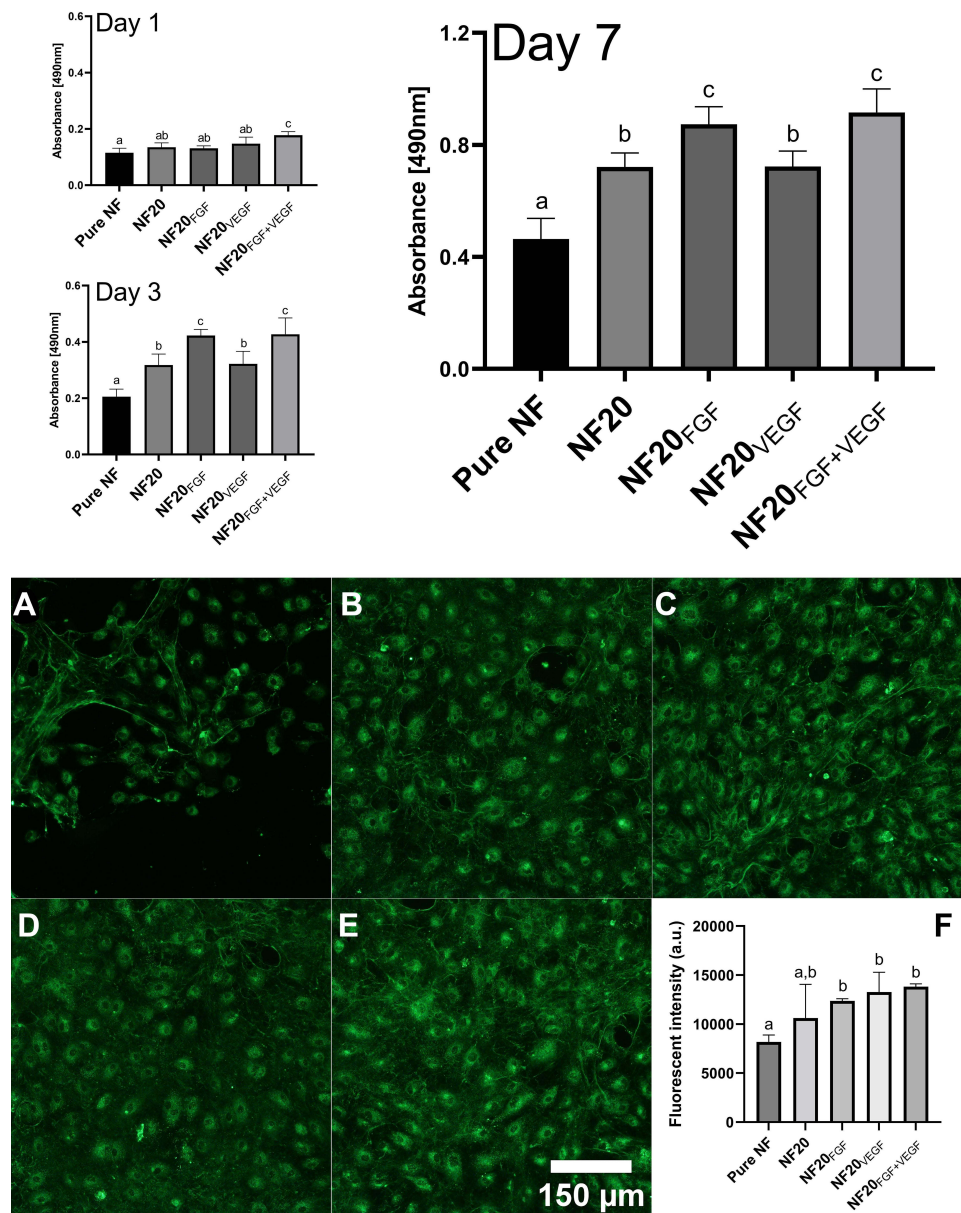


Figure 6 Viability of HSVECs after 1, 3, and 7-day incubation with coated nanofibers. The images of the HSVECs stained with Willebrand factor antibody (green) represent cell maturation on day 7 cultured with NF. (A) uncoated (pure) NF; (B) NF20; (C) NF20_{FGF}; (D) NF20_{VEGF}; (E) NF20_{FGF+VEGF}. Graph (F) represents fluorescence intensity of stained cells. Observed under the Olympus X71 microscope, the intensity was measured by ImageJ. The superscript letters above the columns (a, b, c) denote significant differences between samples that do not share the same superscript ($p < 0.05$).

a wound and stimulate neovascularization in DU. Nevertheless, the combination of VEGF and FGF showed a strong synergistic effect, especially after the first day. The maturation of HSVECs evaluated via immunostaining of the von Willebrand factor (vWF) indicated that cells were able to mature and express the vWF in the presence of the NF. After 7 days, the cells on NF20, NF20_{FGF}, NF20_{VEGF}, and NF20_{FGF+VEGF} had already formed a confluent cell monolayer, while only a few cell islands were observed on uncoated NF. In addition, we observed significant difference in the vWF expression on the samples containing GFs versus pure NF (Figure 6F). Our findings are supported by previously published studies that VEGF and FGF have a positive effect on endothelial cell growth^{17,19,46} as well as on healing wounds³³ in a diabetic mouse model.

Treatment of DU is complicated and limited by the rate of the wound closure and protection against infection. Several other advanced wound dressing strategies based on hydrocolloids, hydrogels, foams, and films incorporating exosomes, nanoparticles, and various bioactive compounds are studied aiming at improved healing by sustained release of

stimulating mediators and drugs, as well as enhanced protection against bacterial infiltration.^{47–51} The combination of biodegradable electrospun blend of PLCL/PCL nanofibers dressings with human platelet lysate and growth factors embedded in a fibrin mesh constitutes a good alternative for the healing of wounds by providing appropriate stimuli in the chronic wound. Importantly, nanofiber scaffolds can mimic ECM and therefore are an ideal material for tissue engineering in the regeneration of damaged skin with a nano-sized structure and a huge surface-to-volume ratio allowing increased loading capacity of the bioactive constituents.⁵ In addition, nanofibers provide also an adequate mechanical protection of the wound.

Conclusion

Wound healing is a dynamic process highly dependent on the overlapping functions of several cell lines such as inflammatory cells, endothelial cells, fibroblasts, and keratinocytes, with the aim of restoring damaged tissue. Considering DU complexity, a chronic wound treatment by a dressing combining delivery of growth factors (GFs) and bioactive molecules from hPL has great potential for DU healing.

In this study, we report functionalization of PLCL/PCL nanofibers (NF) dressings with human platelet lysate and growth factors, ie VEGF and/or FGF, embedded in a fibrin mesh formed in a controlled manner. Coatings formed a uniform protein layer on NF and were characterized by their stability, protein and growth factor content and their release. The highest amount of hPL protein was present in the fibrin mesh with 20% of hPL (NF20). Although a major part of the protein was released from NF20 after one week, results indicated that bioactive molecules such as fibronectin, FGF and VEGF persisted in the coating even after one week due to their specific interaction with the fibrin. The hPL in the coating improved fibrinolytic resistance of the fibrin coating via incorporation of α 2-antiplasmin naturally present in hPL. The coated PLCL/PCL dressing stimulated growth of HSVECs in a model experiment mimicking the wound environment. The highest effect on cell viability was observed for fibrin coated PLCL/PCL nanofibers loaded with 20% of human platelet lysate. Moreover, the addition of FGF and VEGF to the NF20 dressing significantly supported cell proliferation and suggests that the fibrin-based coating combining growth factors and hPL can be used as a promising wound dressing for the clinical treatment of DU. The incorporation of various bioactive molecules from hPL and growth factors has great potential to support the healing processes by providing appropriate stimuli in the chronic wound.

Abbreviations

DU, diabetic ulcers; hPL, human platelet lysate; Fbg, fibrinogen; Thr, thrombin; GFs, growth factors; FGF, fibroblast growth factor 2; VEGF, vascular endothelial growth factor 165; HSVECs, human saphenous vein endothelial cells; ROS, reactive oxygen species; ECM, extracellular matrix; PCL, polycaprolactone; NF, nanofiber membranes; TB, tris buffer; Fn, fibronectin; von Willebrand factor, vWF.

Acknowledgments

This study was supported by the Czech Health Research Council, Ministry of Health of the Czech Republic, project No. NV18-01-00332 and by the project National Institute for Research of Metabolic and Cardiovascular Diseases (Programme EXCELES, ID Project No. LX22NPO5104) - Funded by the European Union - Next Generation EU.

Disclosure

The authors declare that they have no competing interests.

References

1. Gottrup F. A specialized wound-healing center concept: importance of a multidisciplinary department structure and surgical treatment facilities in the treatment of chronic wounds. *Am J Surg*. 2004;187(5):S38–S43. doi:10.1016/S0002-9610(03)00303-9
2. Martino MM, Briquez PS, Maruyama K, Hubbell JA. Extracellular matrix-inspired growth factor delivery systems for bone regeneration. *Adv Drug Deliv Rev*. 2015;94:41–52. doi:10.1016/j.addr.2015.04.007
3. Everett E, Mathioudakis N. Update on management of diabetic foot ulcers. *Ann N Y Acad Sci*. 2018;1411(1):153–165. doi:10.1111/NYAS.13569
4. Zubair M, Ahmad J. Role of growth factors and cytokines in diabetic foot ulcer healing: a detailed review. *Rev Endocr Metab Disord*. 2019;20(2):207–217. doi:10.1007/S11154-019-09492-1

5. Khan A, Morsi Y, Zhu T, et al. Electrospinning: an emerging technology to construct polymer-based nanofibrous scaffolds for diabetic wound healing. *Front Mater Sci.* **2021**;15(1):10–35. doi:10.1007/S11706-021-0540-1
6. Woodruff MA, Hutmacher DW. The return of a forgotten polymer—Polycaprolactone in the 21st century. *Prog Polym Sci.* **2010**;35(10):1217–1256. doi:10.1016/J.PROGPOLYMSCI.2010.04.002
7. Miguel SP, Sequeira RS, Moreira AF, et al. An overview of electrospun membranes loaded with bioactive molecules for improving the wound healing process. *Eur J Pharm Biopharm.* **2019**;139:1–22. doi:10.1016/J.EJPB.2019.03.010
8. Bonferoni MC, Rossi S, Sandri G, et al. Bioactive medications for the delivery of platelet derivatives to skin wounds. *Curr Drug Deliv.* **2019**;16(5):472–483. doi:10.2174/1381612825666190320154406
9. O'Connell SM, Impeduglia T, Hessler K, Wang XJ, Carroll RJ, Dardik H. Autologous platelet-rich fibrin matrix as cell therapy in the healing of chronic lower-extremity ulcers. *Wound Repair Regen.* **2008**;16(6):749–756. doi:10.1111/J.1524-475X.2008.00426.X
10. Sovkova V, Vocetkova K, Rampichova M, et al. Platelet lysate as a serum replacement for skin cell culture on biomimetic PCL nanofibers. *Platelets.* **2017**;29(4):395–405. doi:10.1080/09537104.2017.1316838
11. Chiara Barsotti M, Losi P, Briganti E, et al. Effect of platelet lysate on human cells involved in different phases of wound healing. *PLoS One.* **2013**;8(12):e84753. doi:10.1371/journal.pone.0084753
12. Jafar H, Hasan M, Al-Hattab D, et al. Platelet lysate promotes the healing of long-standing diabetic foot ulcers: a report of two cases and in vitro study. *Heliyon.* **2020**;6(5):e03929. doi:10.1016/J.HELİYON.2020.E03929
13. Weisel JW, Litvinov RI. Fibrin Formation, Structure and Properties. *Subcell Biochem.* **2017**;82:405–456. doi:10.1007/978-3-319-49674-0_13
14. Sahni A, Francis CW. Vascular endothelial growth factor binds to fibrinogen and fibrin and stimulates endothelial cell proliferation. *Blood.* **2000**;96(12):3772–3778. doi:10.1182/blood.v96.12.3772.h8003772_3772_3778
15. Sahni A, Odrliin T, Francis CW. Binding of basic fibroblast growth factor to fibrinogen and fibrin. *J Biol Chem.* **1998**;273(13):7554–7559. doi:10.1074/JBC.273.13.7554
16. Bacakova M, Musilkova J, Riedel T, et al. The potential applications of fibrin-coated electrospun polylactide nanofibers in skin tissue engineering. *Int J Nanomedicine.* **2016**;11:771–789. doi:10.2147/IJN.S99317
17. Blanquer A, Musilkova J, Filova E, et al. The Effect of a Polyester Nanofibrous Membrane with a Fibrin-Platelet Lysate Coating on Keratinocytes and Endothelial Cells in a Co-Culture System. *Nanomater.* **2021**;11(2):457. doi:10.3390/NANO11020457
18. Tan P, Chan C, Xue S, et al. Phenotypic and functional differences between human saphenous vein (HSVEC) and umbilical vein (HUVEC) endothelial cells. *Atherosclerosis.* **2004**;173(2):171–183. doi:10.1016/J.ATHEROSCLEROSIS.2003.12.011
19. Táborská J, Riedelová Z, Brynda E, Májek P, Riedel T. Endothelialization of an ePTFE vessel prosthesis modified with an antithrombogenic fibrin/heparin coating enriched with bound growth factors. *RSC Adv.* **2021**;11(11):5903–5913. doi:10.1039/d1ra00053e
20. Riedel T, Brynda E, Dyr JE, Houska M. Controlled preparation of thin fibrin films immobilized at solid surfaces. *J Biomed Mater Res Part A.* **2009**;88A(2):437–447. doi:10.1002/jbm.a.31755
21. Augustine R, Dominic EA, Reju I, Kaimal B, Kalarikkal N, Thomas S. Electrospun poly(ϵ -caprolactone)-based skin substitutes: in vivo evaluation of wound healing and the mechanism of cell proliferation. *J Biomed Mater Res Part B Appl Biomater.* **2015**;103(7):1445–1454. doi:10.1002/JBM.B.33325
22. Jeong SI, Jun ID, Choi MJ, Nho YC, Lee YM, Shin H. Development of electroactive and elastic nanofibers that contain polyaniline and poly(L-lactide-co- ϵ -caprolactone) for the control of cell adhesion. *Macromol Biosci.* **2008**;8(7):627–637. doi:10.1002/MABI.200800005
23. Riedelová-Reichelová Z, Brynda E, Riedel T. Fibrin nanostructures for biomedical applications. *Physiol Res.* **2016**;65(S2):S263–S272. doi:10.33549/physiolres.933428
24. Perttilä J, Salo M, Peltola O. Plasma fibronectin concentrations in blood products. *Intensive Care Med.* **1990**;16(1):41–43. doi:10.1007/BF01706323
25. Lenselink EA. Role of fibronectin in normal wound healing. *Int Wound J.* **2015**;12(3):313–316. doi:10.1111/IWJ.12109
26. Martino MM, Briquez PS, Ranga A, Lutolf MP, Hubbell JA. Heparin-binding domain of fibrin(ogen) binds growth factors and promotes tissue repair when incorporated within a synthetic matrix. *Proc Natl Acad Sci.* **2013**;110(12):4563. doi:10.1073/PNAS.1221602110
27. Johnson MB, Pang B, Gardner DJ, et al. Topical fibronectin improves wound healing of irradiated skin. *Sci Rep.* **2017**;7(1):3876. doi:10.1038/S41598-017-03614-Y
28. Qiu Z, Kwon AH, Kamiyama Y. Effects of plasma fibronectin on the healing of full-thickness skin wounds in streptozotocin-induced diabetic rats. *J Surg Res.* **2007**;138(1):64–70. doi:10.1016/J.JSS.2006.06.034
29. Abdul S, Leebeck FWG, Rijken DC, De Willige SU. Natural heterogeneity of α 2-antiplasmin: functional and clinical consequences. *Blood.* **2016**;127(5):538–545. doi:10.1182/BLOOD-2015-09-670117
30. Tsurupa G, Yakovlev S, McKee P, Medved L. Noncovalent interaction of α (2)-antiplasmin with fibrin(ogen): localization of α (2)-antiplasmin-binding sites. *Biochemistry.* **2010**;49(35):7643–7651. doi:10.1021/BI1010317
31. Sulniute R, Shen Y, Guo Y-Z, et al. Plasminogen is a critical regulator of cutaneous wound healing. *Thromb Haemost.* **2017**;116(05):1001–1009. doi:10.1160/TH15-08-0653
32. Hoffman R, Starkey S, Coad J. Wound fluid from venous leg ulcers degrades plasminogen and reduces plasmin generation by keratinocytes. *J Invest Dermatol.* **1998**;111(6):1140–1144. doi:10.1046/J.1523-1747.1998.00429.X
33. Losi P, Al KT, Buscemi M, Foffa I, Cavallo A, Soldani G. Bilayered fibrin-based electrospun-sprayed scaffold loaded with platelet lysate enhances wound healing in a diabetic mouse model. *Nanomater.* **2020**;10(11):2128. doi:10.3390/NANO10112128
34. Sahni A, Baker CA, Sporn LA, Francis CW. Fibrinogen and fibrin protect fibroblast growth factor-2 from proteolytic degradation. *Thromb Haemost.* **2000**;83(5):736–741. doi:10.1055/S-0037-1613902
35. Crafts TD, Jensen AR, Blocher-Smith EC, Markel TA. Vascular endothelial growth factor: therapeutic possibilities and challenges for the treatment of ischemia. *Cytokine.* **2015**;71(2):385–393. doi:10.1016/J.CYTO.2014.08.005
36. Park JW, Hwang SR, Yoon IS. Advanced growth factor delivery systems in wound management and skin regeneration. *Molecules.* **2017**;22:8. doi:10.3390/MOLECULES22081259
37. Galiano RD, Tepper OM, Pelo CR, et al. Topical vascular endothelial growth factor accelerates diabetic wound healing through increased angiogenesis and by mobilizing and recruiting bone marrow-derived cells. *Am J Pathol.* **2004**;164(6):1935–1947. doi:10.1016/S0002-9440(10)63754-6

38. Barrientos S, Brem H, Stojadinovic O, Tomic-Canic M. Clinical application of growth factors and cytokines in wound healing. *Wound Repair Regen.* 2014;22(5):569–578. doi:10.1111/WRR.12205
39. Certelli A, Valente P, Uccelli A, et al. Robust Angiogenesis and Arteriogenesis in the Skin of Diabetic Mice by Transient Delivery of Engineered VEGF and PDGF-BB Proteins in Fibrin Hydrogels. *Front Bioeng Biotechnol.* 2021;9:688467. doi:10.3389/fbioe.2021.688467
40. Hanft JR, Pollak RA, Barbul A, et al. Phase I trial on the safety of topical rhVEGF on chronic neuropathic diabetic foot ulcers. *J Wound Care.* 2008;17(1):30–2,34–7. doi:10.12968/JOWC.2008.17.1.27917
41. Marti-Carvajal AJ, Gluud C, Nicola S, et al. Growth factors for treating diabetic foot ulcers. *Cochrane Database Syst Rev.* 2015;2015(10):CD008548. doi:10.1002/14651858.CD008548.PUB2
42. Greenhalgh DG, Sprugel KH, Murray MJ, Ross R. PDGF and FGF stimulate wound healing in the genetically diabetic mouse. *Am J Pathol.* 1990;136(6):1235.
43. Akita S, Akino K, Imaizumi T, Hirano A. Basic fibroblast growth factor accelerates and improves second-degree burn wound healing. *Wound Repair Regen.* 2008;16(5):635–641. doi:10.1111/J.1524-475X.2008.00414.X
44. Lerman OZ, Galiano RD, Armour M, Levine JP, Gurtner GC. Cellular dysfunction in the diabetic fibroblast: impairment in migration, vascular endothelial growth factor production, and response to hypoxia. *Am J Pathol.* 2003;162(1):303–312. doi:10.1016/S0002-9440(10)63821-7
45. Thangarajah H, Yao D, Chang EI, et al. The molecular basis for impaired hypoxia-induced VEGF expression in diabetic tissues. *Proc Natl Acad Sci.* 2009;106(32):13505–13510. doi:10.1073/PNAS.0906670106
46. Cross MJ, Claesson-Welsh L. FGF and VEGF function in angiogenesis: signalling pathways, biological responses and therapeutic inhibition. *Trends Pharmacol Sci.* 2001;22(4):201–207. doi:10.1016/S0165-6147(00)01676-X
47. Chiu A, Sharma D, Zhao F. Tissue Engineering-Based Strategies for Diabetic Foot Ulcer Management. *Adv Wound Care.* 2023;12(3):145–167. doi:10.1089/wound.2021.0081
48. Zhang S, Ge G, Qin Y, et al. Recent advances in responsive hydrogels for diabetic wound healing. *Mater Today Bio.* 2023;18:100508. doi:10.1016/j.mtbio.2022.100508
49. Chen Z, Wu H, Wang H, et al. An injectable anti-microbial and adhesive hydrogel for the effective noncompressible visceral hemostasis and wound repair. *Mater Sci Eng.* 2021;129:112422. doi:10.1016/j.msec.2021.112422
50. Li J, Gao H, Xiong Y, et al. Enhancing Cutaneous Wound Healing Based on Human Induced Neural Stem Cell-derived Exosomes. *Int J Nanomedicine.* 2022;17:5991–6006. doi:10.2147/IJN.S377502
51. Qin W, Wu Y, Liu J, et al. A Comprehensive Review of the Application of Nanoparticles in Diabetic Wound Healing: therapeutic Potential and Future Perspectives. *Int J Nanomedicine.* 2022;17:6007–6029. doi:10.2147/IJN.S386585

International Journal of Nanomedicine

Dovepress

Publish your work in this journal

The International Journal of Nanomedicine is an international, peer-reviewed journal focusing on the application of nanotechnology in diagnostics, therapeutics, and drug delivery systems throughout the biomedical field. This journal is indexed on PubMed Central, MedLine, CAS, SciSearch®, Current Contents®/Clinical Medicine, Journal Citation Reports/Science Edition, EMBase, Scopus and the Elsevier Bibliographic databases. The manuscript management system is completely online and includes a very quick and fair peer-review system, which is all easy to use. Visit <http://www.dovepress.com/testimonials.php> to read real quotes from published authors.

Submit your manuscript here: <https://www.dovepress.com/international-journal-of-nanomedicine-journal>